NANO LETTERS

Letter

pubs.acs.org/NanoLett

An Advanced Lithium–Air Battery Exploiting an Ionic Liquid-Based Electrolyte

G. A. Elia,[†] J. Hassoun,*[,†] W.-J. Kwak,[‡] Y.-K. Sun,*[,‡] B. Scrosati,*[,§] F. Mueller,[∥,⊥] D. Bresser,[∥,⊥] S. Passerini,*[,∥,⊥] P. Oberhumer,[#] N. Tsiouvaras,[#] and J. Reiter[#]

[†]Chemistry Department, University of Rome - La Sapienza, 00185 Rome, Italy

[‡]Department of Energy Engineering, Hanyang University, Seoul 133-791, South Korea

[§]Elettrochimica ed Energia, 00199 Rome, Italy

[∥]Electrochemistry I, Helmholtz-Institute Ulm, 89081 Ulm, Germany

[⊥]Karlsruher Institute of Technology, 76344 Eggenstein-Leopoldshafen, Germany

[#]BMW Group, 80788 Munich, Germany

Supporting Information

ABSTRACT: A novel lithium–oxygen battery exploiting $PYR_{14}TFSI$–LiTFSI as ionic liquid-based electrolyte medium is reported. The Li/$PYR_{14}TFSI$–LiTFSI/O_2 battery was fully characterized by electrochemical impedance spectroscopy, capacity-limited cycling, field emission scanning electron microscopy, high-resolution transmission electron microscopy, and X-ray photoelectron spectroscopy. The results of this extensive study demonstrate that this new Li/O_2 cell is characterized by a stable electrode–electrolyte interface and a highly reversible charge–discharge cycling behavior. Most remarkably, the charge process (oxygen oxidation reaction) is characterized by a very low overvoltage, enhancing the energy efficiency to 82%, thus, addressing one of the most critical issues preventing the practical application of lithium–oxygen batteries.

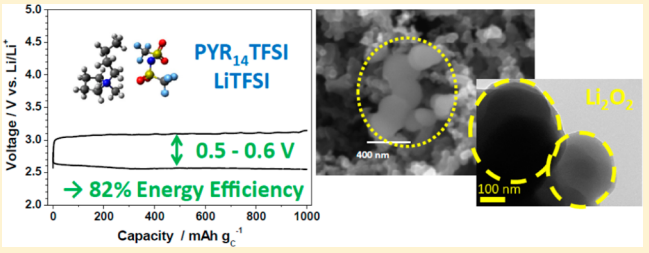

KEYWORDS: *Li–O_2 cell, ionic liquid, electrolyte, energy efficiency, lithium–oxygen battery*

In the course of the past decade, due to its high theoretical energy density assumed to be comparable to that of gasoline, the lithium–air battery has attracted great attention of many academic and industrial laboratories worldwide.[1−6] However, the practical development of this battery is still hindered by various issues including (i) the poor reversibility of the lithium–oxygen electrochemical process,[7−9] (ii) the low energy storage efficiency caused by the rather high polarization resulting in a wide charge–discharge voltage gap,[10,11] (iii) the reactivity and therefore poor stability of commonly used organic electrolytes both at the lithium side and, in particular, at the oxygen side,[12−14] and (iv) the sensitivity of the system to CO_2 and H_2O contamination, requiring the use of pure oxygen rather than air as the feeding source.[15−17]

Recently, some progress was obtained in the understanding of the lithium–oxygen reaction mechanism in nonaqueous media,[18,19] the identification of a stable electrolyte in the cell environment,[20−24] and the demonstration of an alternative lithium metal-free concept using Si–C composite as anode material.[25] However, the low energy efficiency and severe safety concerns associated with the reactivity of the lithium metal anode remain still unsolved and prevent the practical application of the lithium–oxygen battery technology. Accordingly, the development of a lithium–oxygen cell that combines a sufficiently high energy efficiency and suitable safety even for large-scale devices presents a mandatory step toward its targeted commercialization in future.

Herein, we report a new step forward toward the realization of commercial lithium–oxygen batteries, consisting in the development of a Li/O_2 cell exploiting an ionic liquid (IL)-based (specifically, *N*-butyl-*N*-methylpyrrolidinium bis(trifluoromethanesulfonyl)imide–lithium bis(trifluoromethanesulfonyl)imide, $PYR_{14}TFSI$–LiTFSI) electrolyte. This electrolyte was chosen due to its well-known nonflammable nature, high electrochemical stability versus the superoxide formation,[26] and chemical inertness combined with a thermal stability of up to a 300–400 °C,[27−29] that is, features that are expected to address the previously mentioned safety issues.

The use of ionic liquid-based electrolytes in Li-oxygen cells was already discussed in literature[28−33] and very recently reviewed by Bresser et al.[34] For instance, Mastragostino and co-workers,[28] studied the utilization of $PYR_{14}TFSI$–LiTFSI (9:1 molar ratio) in a new Li-oxygen cell configuration in which the oxygen-saturated electrolyte is circulated through the cell.

Received: August 20, 2014
Revised: October 8, 2014
Published: October 20, 2014

   dx.doi.org/10.1021/nl5031985 | *Nano Lett.* 2014, 14, 6572–6577

Nevertheless, the reversibility of the (dis-)charge process remained poor, presumably related to a dramatic increase of the lithium metal overpotential, caused by the formation of an insulating film on the surface. In a later study, they reported the utilization of a catalyst-free, porous, carbonaceous oxygen electrode in a rather simple cell configuration (5 mL cell), bubbling oxygen through the cell.[32] Remarkably, the charge potential was lowered to about 3.4 V but the obtained specific capacity remained rather poor (200 mAh g^{-1}) accompanied by a rather low Coulombic efficiency. Abraham and co-workers investigated the oxygen reduction and evolution reaction in ionic liquids in the presence of lithium ions, reporting a reversible capacity of around 1800 mAh g^{-1} and, again, a rather low charge potential of about 3.4 V.[29,30] However, no continuous cycling of the cell was reported. In fact, all studies on lithium−oxygen batteries, comprising ionic liquid-based electrolytes, reported so far focused either on basic electrochemical investigations of the oxygen reactions[29,31,32] or were limited to cells showing only few cycles and/or limited capacities.[28,29,31−33]

In this work, we complete the investigation by showing that these electrolytes, when used in proper concentration and cell configuration, may indeed be suitable for operation in a full Li−air battery, offering unique properties in terms of reversibility and particularly energy efficiency due to a reduced overpotential of the oxygen evolution reaction (OER).

The electrochemical performance of the Li/PYR_{14}TFSI−LiTFSI/O_2 battery was first evaluated by capacity-limited galvanostatic cycling (see Methods section in the Supporting Information for details) using the coin-cell experimental setup reported in the Supporting Information (Figure S1). Figure 1a shows the corresponding voltage profiles and Figure 1b the electrochemical impedance spectra obtained at various cycling stages. The discharge and charge voltages, corresponding to the formation and dissolution of the Li_2O_2 particles, respectively, are centered at 2.6 and 3.2 V versus Li/Li^+ (Figure 1a), resulting in an overall cell polarization value limited to only 0.6 V, that is, a particular remarkably low value, considering that it was obtained with a catalyst-free electrode (named GDL-SP) composed of a commercial gas diffusion layer (GDL) coated with carbon black. We propose that the large improvement in reducing the cell polarization may be explained in light of the fact that the discharge in the ionic liquid electrolyte leads to the formation of lithium peroxide particles having a much smaller size than that usually observed in other electrolyte media, this finally allowing a facile reconversion and, hence, a low polarization overvoltage. It has to be stressed that this low discharge−charge gap results in an energy efficiency in the order of 82%, that is, a value rarely met in previous Li−O_2 battery studies. The occurrence of unwanted side reactions during the charge process cannot be totally excluded as discussed later on. However, in the ideal case, considering the full reversibility of the reaction, the voltage should remain constant upon charge for capacity-limited cycling, as observed in Figure 1a. Moreover, the inset of Figure 1a evidences a stable cycling behavior, thus, excluding that these reactions may induce significant electrolyte degradation upon operation. The stability of the ionic liquid-based electrolyte is further confirmed by the trend of the EIS Nyquist plots determined in the course of continuous cycling (Figure 1b), showing that the battery benefits of a stable electrode/electrolyte interface and an overall low resistance of around 40 Ω, with minor changes most likely associated with solid electrolyte interphase

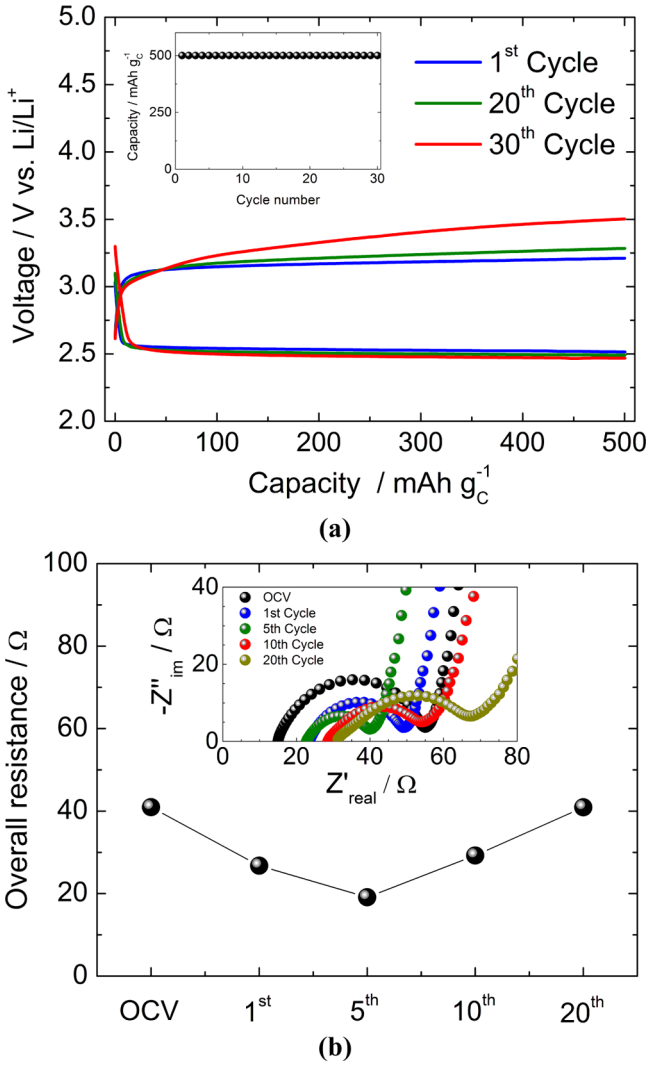

Figure 1. (a) Voltage profiles of the Li/O_2 battery galvanostatically cycled applying a specific current of 50 mA g^{-1} limiting the capacity to 500 mAh g^{-1}. The inset shows the cycling trend; (b) time evolution of the cell interface resistance upon cycling and the related impedance spectra obtained in a frequency range of 75 kHz to 0.1 Hz (inset); electrolyte, PYR_{14}TFSI−LiTFSI; temperature, 30 °C.

(SEI) film formation/dissolution and final stabilization, that is, a behavior typically observed in the common lithium and lithium-ion batteries.[35]

The Li/PYR_{14}TFSI−LiTFSI/O_2 battery was further investigated by using various complementary techniques, including field emission scanning electron microscopy (FESEM), high-resolution transmission electron microscopy (HRTEM), and selected area electron diffraction (SAED). Figure 2 shows the SEM images of the GDL-SP cathode collected at the pristine (Figure 2b, SEM 1), fully discharged (Figure 2c, SEM 2), and fully charged state (Figure 2d, SEM 3, see also Figure 2a for the cycling conditions). We notice that the typical morphology of the pristine GDL-SP electrode (SEM 1) changes upon discharge by revealing the occurrence of Li_2O_2 particles (evidenced by the yellow circle in SEM 2), having a spherical shape, to then return back to the initial state upon charge (SEM 3). These SEM results demonstrate not only the reversibility of the electrochemical process but also provide the first evidence to rationalize the observed low cell polarization.

dx.doi.org/10.1021/nl5031985 | Nano Lett. 2014, 14, 6572−6577

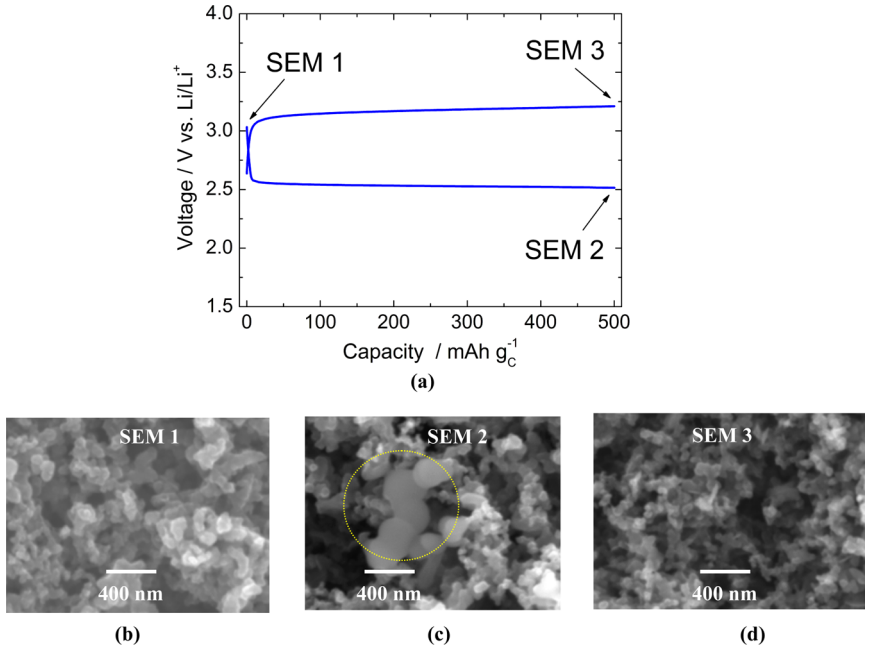

Figure 2. (a) Voltage profile of the Li/O_2 battery galvanostatically cycled applying a specific current of 50 mA g^{-1} and a fixed capacity regime of 500 mAh g^{-1}; FESEM images of the GDL-SP electrode in its pristine state (b), after discharge (c), and after the following charge (d); electrolyte, $PYR_{14}TFSI–LiTFSI$; temperature, 30 °C.

In fact, SEM 2 reveals that the formed Li_2O_2 particles are very small, that is, in the order of 200 nm, hence, expected to be easily dissolved and reformed in the course of the charge–discharge cycling process. As explanation of this phenomenon, we may assume that the size of the formed Li_2O_2 particles depends on the diffusion of lithium in the electrolyte media, which in ionic liquids is expected to be lower than in other electrolytes. As a matter of fact, lithium ion diffusion-limited conditions would favor nucleation rather than crystal growth, resulting in the formation of many but smaller Li_2O_2 particles rather than less and bigger particles.

The SEM analysis was further extended to a full-capacity charge–discharge cycle performed applying specific cutoff voltages rather than the capacity limitation, resulting in a specific capacity of about 4500 mAh g_{carbon}^{-1} referring to the SP carbon loading (0.8 mg cm^{-2}) and corresponding to an area-normalized capacity of about 4 mA cm_{carbon}^{-2} (see Figure 3a). A cell polarization slightly higher than under capacity-limited conditions (compare Figures 1a and 2a) is observed here in particular at the final part of the charging process. This is most likely related to a progressive agglomeration of the lithium peroxide particles upon the prolonged discharge time, as in fact confirmed by the comparison with the cathode SEM images of cells discharged to 500 mAh g_{carbon}^{-1} (Figure 3b,c).[36] It appears noteworthy, however, that the Coulombic efficiency remains high, that is, about 98.5%, confirming a very good reversibility of the electrochemical process, that is, the lithium peroxide formation is assured even under this high capacity cycling regime.

Figure 4 shows the HRTEM analysis of the GDL-SP cathode obtained in the course of the discharge process of the $Li/PYR_{14}TFSI–LiTFSI/O_2$ battery as well as the corresponding selected area electron diffraction (SAED) patterns. The results reveal lithium peroxide particles with an average size of about 200 nm (Figure 4a–c), confirming the results obtained by means of SEM analysis (compare with Figure 2b). It should be noted that the particles are amorphous (see Figure 4d), which is presumably related to the kinetics of Li_2O_2 formation in $PYR_{14}TFSI–LiTFSI$, and that they are smaller than those formed in Li/O_2 cells using the conventional tetraglyme-based electrolyte (see Supporting Information Figure S2a,b, reporting the comparison of TEM images of particles formed in $PYR_{14}TFSI–LiTFSI$ and TEGDME–LiTFSI (1:4 molar ratio) and Supporting Information Figure S3 comparing the

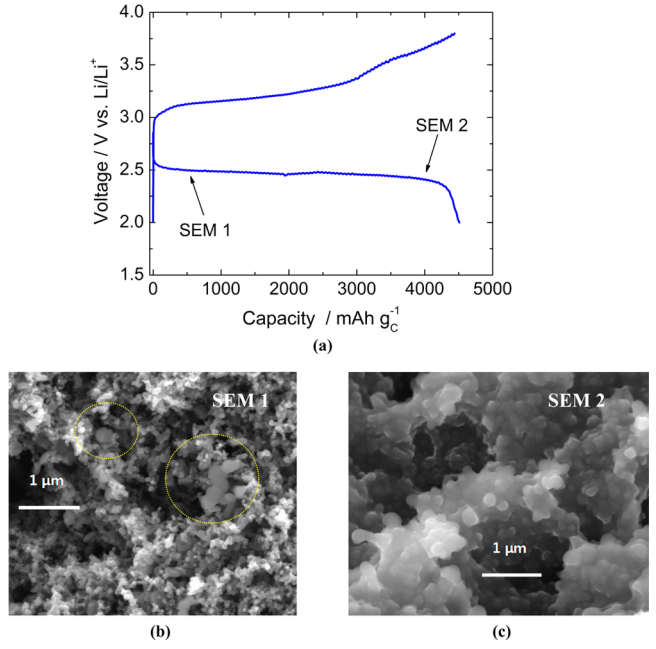

Figure 3. (a) Voltage profile of the lithium–oxygen cell galvanostatically cycled applying a current of 100 mA g^{-1} in the 2.0–3.8 V voltage range without capacity limitation; FESEM images of the GDL-SP electrode upon discharge at 500 (b) and 4000 mAh g^{-1} (c); electrolyte, $PYR_{14}TFSI–LiTFSI$; temperature, 30 °C.

dx.doi.org/10.1021/nl5031985 | Nano Lett. 2014, 14, 6572–6577

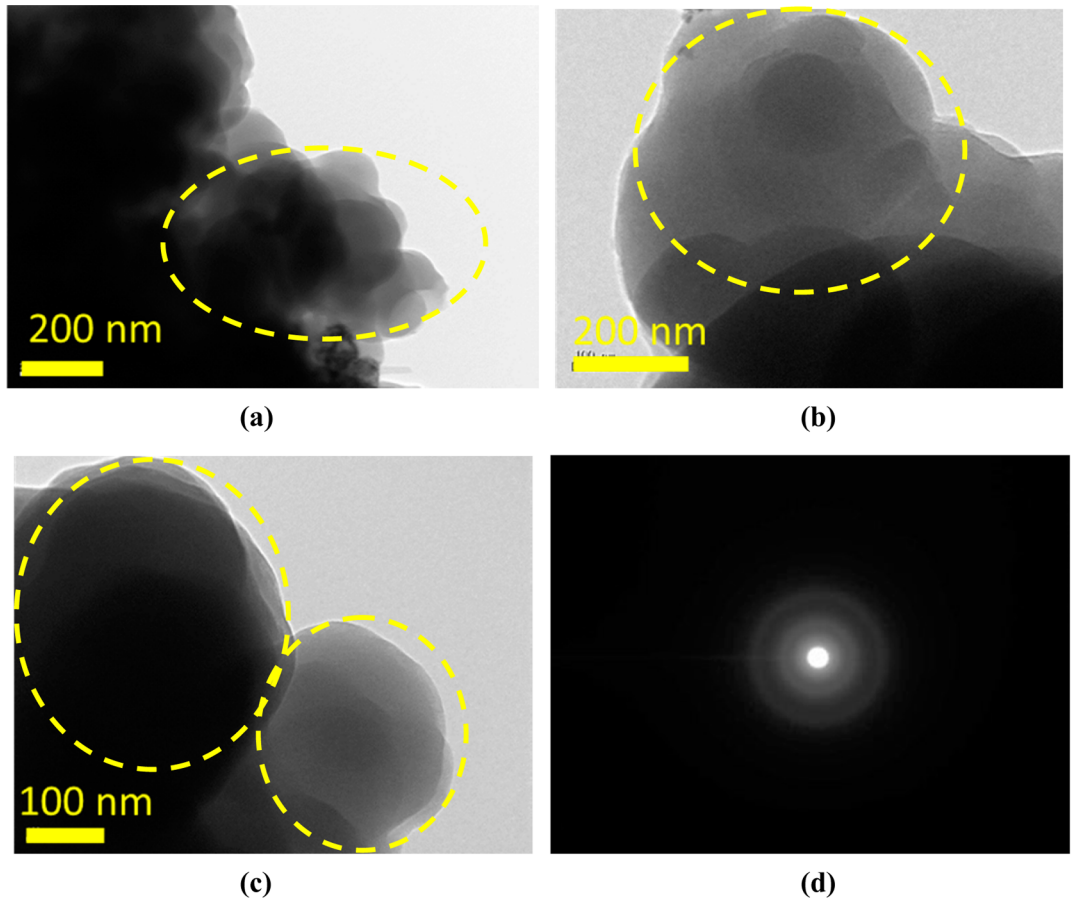

Figure 4. (a–c) HRTEM images of the GDL-SP electrode at various magnifications upon discharge at 4000 mAh g^{-1} and (d) the corresponding selected area electron diffraction (SAED) patterns. The formed Li_2O_2 particles are marked by yellow cycles. Electrolyte, $PYR_{14}TFSI–LiTFSI$; temperature, 30 °C.

XRD patterns of the discharged cathode after cycling in our IL-based cell with that of a similar cell cycled in TEGDME–$LiCF_3SO_3$).[21] This evidence accounts for the major difference in charge overpotential observed in the two cases (see Supporting Information Figure S2c, reporting the comparison of cell behavior in $PYR_{14}TFSI–LiTFSI$ and TEGDME-$LiCF_3SO_3$) and provides an additional support to rationalize the high energy efficiency obtained with the ionic liquid-based battery reported in this work.

The reversibility of the $2\ Li^+ + 2\ e^- + O_2 \leftrightarrows Li_2O_2$ electrochemical process of the $Li/PYR_{14}TFSI–LiTFSI/O_2$ battery was finally examined by ex situ XPS analysis of GDL-SP electrodes at the final stages of its charge and discharge process. Figure 5b shows the results. Nevertheless, the Li 1s peak assigned to Li_2O_2 is still detectable after the charge, thus suggesting a slight incompleteness of the charging process, confirming that a minor occurrence of side reactions cannot be excluded. However, it is important to stress that the good reversibility combined with the superior energy efficiency (see Figure 5a) is obtained for cycling the cell at a capacity of 1000 mAh g_{carbon}^{-1}, namely at the regime commonly used for testing Li/O_2 cells.[21,36] Finally, we have checked the stability of PVdF because it has been reported that this binder may decompose in the presence of superoxide.[37] XPS analysis has confirmed that this is not the case for our IL-based battery (see Supporting Information Figure S4). We assume that this different result is related to the fact that our battery operates in a different electrolyte medium, which is known to stabilize the superoxide anion radical.[26]

Although, this is not the first work reporting the use of ionic liquid-based electrolytes in $Li–O_2$ cells, which were, in fact, discussed in previous studies, it is certainly the first in demonstrating that these electrolytes are suitable for operation in a full $Li–O_2$ battery, offering unique properties in terms of reversibility and particularly energy efficiency. We suppose that the favorable performance of our battery, and particularly its capability of cycling with a low charging overpotential, reflecting in a value of energy density rarely met in the past, is directly linked to the properties of the electrolyte medium and in particular to its transport properties. In addition, we assume that the choice of the appropriate cell design contributed to the results reported herein. We show in fact, that the discharge ORR process in the herein utilized $PYR_{14}TFSI–LiTFSI$ electrolyte leads to lithium peroxide particles having a size much smaller than that usually obtained in other media, this finally allowing a facile reconversion in the charge OER process. We are currently extending our investigation to other ionic liquids to achieve a more detailed understanding of the role of this class of electrolytes in the $Li–O_2$ battery chemistry. Although not specifically demonstrated in this work, it is reasonable to assume that the high thermal stability of the IL-based electrolyte can offer the additional bonus of enhancing the safety of the battery. It may then be concluded that the results reported in this work are of importance for the progress of the Li/O_2 electrochemical

dx.doi.org/10.1021/nl5031985 | *Nano Lett.* 2014, 14, 6572–6577

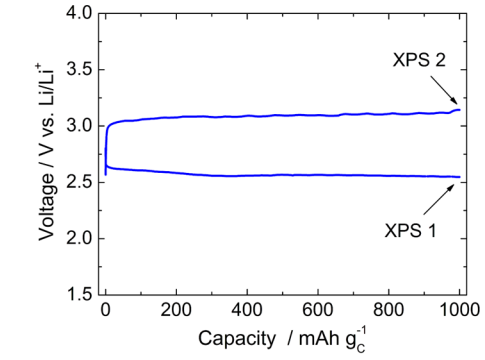

(a)

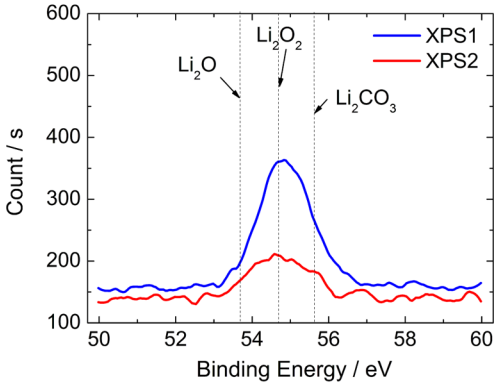

(b)

Figure 5. (a) Voltage profile of the lithium oxygen cell galvanostatically cycled applying a current of 100 mA g^{-1} and a capacity limited to 1000 mAh g^{-1} and (b) Li 1s XPS spectra of the GDL-SP electrode at the end of discharge (blue curve) and after the following charge (red curve); electrolyte, $PYR_{14}TFSI-LiTFSI$; temperature, 30 °C.

system by contributing to promote its practical evolution as power source of choice for the sustainable, electrified road transportation.

■ ASSOCIATED CONTENT

Supporting Information

Detailed description of the materials and methods used herein. A photograph of the utilized cell setup is presented (Figure S1) as well as a comparative TEM and XRD study of $Li-O_2$ cells comprising $PYR_{14}TFSI-LiTFSI$ and $TEGDME-LiCF_3SO_3$ (Figures S2 and S3). Finally, the XPS analysis of the (dis-)charged oxygen cathode is included, confirming the stability of the PVdF binder (Figure S4). This material is available free of charge via the Internet at http://pubs.acs.org

■ AUTHOR INFORMATION

Corresponding Authors

*E-mail: (J.H.) jusef.hassoun@uniroma1.it.
*E-mail: (Y.-K.S.) yksun@hanyang.ac.kr.
*E-mail: (B.S.) bruno.scrosati@gmail.com.
*E-mail: (S.P.) stefano.passerini@kit.edu.

Notes

The authors declare no competing financial interest.

■ ACKNOWLEDGMENTS

This work was financially supported by BMW AG within the ABILE (Air Batteries with Ionic Liquid Electrolytes) project. The authors would like to thank Dr. Sangsik Jeong for synthesizing the ionic liquid. Y.-K.S. and W.-J.K. acknowledge the Human Resources Development program (No. 20124010203310) of the Korea Institute of Energy Technology Evaluation and Planning (KETEP) grant funded by the Korea government Ministry of Trade, Industry, and Energy.

■ REFERENCES

(1) Scrosati, B.; Hassoun, J.; Sun, Y.-K. *Energy Environ. Sci.* **2011**, *4*, 3287−3295.
(2) Girishkumar, G.; McCloskey, B.; Luntz, A. C.; Swanson, S.; Wilcke, W. *J. Phys. Chem. Lett.* **2010**, *1*, 2193−2203.
(3) Shao, Y.; Ding, F.; Xiao, J.; Zhang, J.; Xu, W.; Park, S.; Zhang, J.-G.; Wang, Y.; Liu, J. *Adv. Funct. Mater.* **2013**, *23*, 987−1004.
(4) Bruce, P. G.; Freunberger, S. A.; Hardwick, L. J.; Tarascon, J.-M. *Nat. Mater.* **2012**, *11*, 19−29.
(5) Zhang, J.-G.; Bruce, P. G.; Zhang, X. G. In *Handbook of Battery Materials*; Daniel, C., Besenhard, J. O., Eds.; Wiley-VCH: Weinheim, Germany, 2011; pp 757−795.
(6) Hou, J.; Yang, M.; Ellis, M. W.; Moore, R. B.; Yi, B. *Phys. Chem. Chem. Phys.* **2012**, *14*, 13487−13501.
(7) Xu, W.; Viswanathan, V. V.; Wang, D.; Towne, S. A.; Xiao, J.; Nie, Z.; Hu, D.; Zhang, J.-G. *J. Power Sources* **2011**, *196*, 3894−3899.
(8) McCloskey, B. D.; Speidel, A.; Scheffler, R.; Miller, D. C.; Viswanathan, V.; Hummelshøj, J. S.; Nørskov, J. K.; Luntz, A. C. *J. Phys. Chem. Lett.* **2012**, *3*, 997−1001.
(9) Xiao, J.; Hu, J.; Wang, D.; Hu, D.; Xu, W.; Graff, G. L.; Nie, Z.; Liu, J.; Zhang, J.-G. *J. Power Sources* **2011**, *196*, 5674−5678.
(10) Zhang, S. S.; Foster, D.; Read, J. *J. Power Sources* **2010**, *195*, 1235−1240.
(11) Freunberger, S. A.; Chen, Y.; Peng, Z.; Griffin, J. M.; Hardwick, L. J.; Bardé, F.; Novák, P.; Bruce, P. G. *J. Am. Chem. Soc.* **2011**, *133*, 8040−8047.
(12) McCloskey, B. D.; Bethune, D. S.; Shelby, R. M.; Girishkumar, G.; Luntz, A. C. *J. Phys. Chem. Lett.* **2011**, *2*, 1161−1166.
(13) Bryantsev, V. S.; Giordani, V.; Walker, W.; Blanco, M.; Zecevic, S.; Sasaki, K.; Uddin, J.; Addison, D.; Chase, G. V. *J. Phys. Chem. A* **2011**, *115*, 12399−12409.
(14) Bryantsev, V. S.; Faglioni, F. *J. Phys. Chem. A* **2012**, *116*, 7128−7138.
(15) Gowda, S. R.; Brunet, A.; Wallraff, G. M.; McCloskey, B. D. *J. Phys. Chem. Lett.* **2012**, *4*, 276−279.
(16) Zhang, T.; Zhou, H. *Nat. Commun.* **2013**, *4*, 1817.
(17) Crowther, O.; Salomon, M. *Membranes* **2012**, *2*, 216−227.
(18) Leskes, M.; Drewett, N. E.; Hardwick, L. J.; Bruce, P. G.; Goward, G. R.; Grey, C. P. *Angew. Chem.* **2012**, *124*, 8688−8691.
(19) Hassoun, J.; Croce, F.; Armand, M.; Scrosati, B. *Angew. Chem., Int. Ed.* **2011**, *50*, 2999−3002.
(20) Chen, X. J.; Shellikeri, A.; Wu, Q.; Zheng, J. P.; Hendrickson, M.; Plichta, E. J. *J. Electrochem. Soc.* **2013**, *160*, A1619−A1623.
(21) Jung, H.-G.; Hassoun, J.; Park, J.-B.; Sun, Y.-K.; Scrosati, B. *Nat. Chem.* **2012**, *4*, 579−585.
(22) Du, P.; Lu, J.; Lau, K. C.; Luo, X.; Bareno, J.; Zhang, X.; Ren, Y.; Zhang, Z.; Curtiss, L. A.; Sun, Y.-K.; Amine, K. *Phys. Chem. Chem. Phys.* **2013**, *15*, 5572−5581.
(23) Chen, Y.; Freunberger, S. A.; Peng, Z.; Bardé, F.; Bruce, P. G. *J. Am. Chem. Soc.* **2012**, *134*, 7952−7957.
(24) Xu, W.; Hu, J.; Engelhard, M. H.; Towne, S. A.; Hardy, J. S.; Xiao, J.; Feng, J.; Hu, M. Y.; Zhang, J.; Ding, F.; Gross, M. E.; Zhang, J.-G. *J. Power Sources* **2012**, *215*, 240−247.
(25) Hassoun, J.; Jung, H.-G.; Lee, D.-J.; Park, J.-B.; Amine, K.; Sun, Y.-K.; Scrosati, B. *Nano Lett.* **2012**, *12*, 5775−5779.
(26) Randström, S.; Appetecchi, G. B.; Lagergren, C.; Moreno, A.; Passerini, S. *Electrochim. Acta* **2007**, *53*, 1837−1842.
(27) Cecchetto, L.; Salomon, M.; Scrosati, B.; Croce, F. *J. Power Sources* **2012**, *213*, 233−238.
(28) Monaco, S.; Soavi, F.; Mastragostino, M. *J. Phys. Chem. Lett.* **2013**, *4*, 1379−1382.

(29) Allen, C. J.; Hwang, J.; Kautz, R.; Mukerjee, S.; Plichta, E. J.; Hendrickson, M. A.; Abraham, K. M. *J. Phys. Chem. C* **2012**, *116*, 20755−20764.
(30) Allen, C. J.; Mukerjee, S.; Plichta, E. J.; Hendrickson, M. A.; Abraham, K. M. *J. Phys. Chem. Lett.* **2011**, *2*, 2420−2424.
(31) Monaco, S.; Arangio, A. M.; Soavi, F.; Mastragostino, M.; Paillard, E.; Passerini, S. *Electrochim. Acta* **2012**, *83*, 94−104.
(32) Soavi, F.; Monaco, S.; Mastragostino, M. *J. Power Sources* **2013**, *224*, 115−119.
(33) Nakamoto, H.; Suzuki, Y.; Shiotsuki, T.; Mizuno, F.; Higashi, S.; Takechi, K.; Asaoka, T.; Nishikoori, H.; Iba, H. *J. Power Sources* **2013**, *243*, 19−23.
(34) Bresser, D.; Paillard, E.; Passerini, S. *J. Electrochem. Sci. Technol.* **2014**, *5*, 37−44.
(35) Aurbach, D. *J. Power Sources* **2000**, *89*, 206−218.
(36) Jung, H.-G.; Kim, H.-S.; Park, J.-B.; Oh, I.-H.; Hassoun, J.; Yoon, C. S.; Scrosati, B.; Sun, Y.-K. *Nano Lett.* **2012**, *12*, 4333−4335.
(37) Black, R.; Oh, S. H.; Lee, J.-H.; Yim, T.; Adams, B.; Nazar, L. F. *J. Am. Chem. Soc.* **2012**, *134*, 2902−2905.

dx.doi.org/10.1021/nl5031985 | *Nano Lett.* 2014, 14, 6572−6577